

Higher-order shortest paths in hypergraphs

Berné L. Nortier,^{1,*} Simon Dobson,¹ and Federico Battiston^{2,†}

¹ *Department of Computer Science, University of St. Andrews, St. Andrews KY16, Scotland*

² *Department of Network and Data Science, Central European University Vienna, Vienna 1100, Austria*

One of the defining features of complex networks is the connectivity properties that we observe emerging from local interactions. Recently, hypergraphs have emerged as a versatile tool to model networks with non-dyadic, higher-order interactions. Nevertheless, the connectivity properties of real-world hypergraphs remain largely understudied. In this work we introduce path size as a measure to characterise higher-order connectivity and quantify the relevance of non-dyadic ties for efficient shortest paths in a diverse set of empirical networks with and without temporal information. By comparing our results with simple randomised null models, our analysis presents a nuanced picture, suggesting that non-dyadic ties are often central and are vital for system connectivity, while dyadic edges remain essential to connect more peripheral nodes, an effect which is particularly pronounced for time-varying systems. Our work contributes to a better understanding of the structural organisation of systems with higher-order interactions.

INTRODUCTION

Networks, collections of nodes and their interactions, are one of the primary tools used to study complex systems, allowing us to describe collective, emergent system properties which can not be captured by looking at the individual units in isolation [1]. A typical case is the emergence of global connectivity from local interactions, with many real-world networks characterised by the emergence of large connected components [2]. Moreover, such systems display low diameter and are hence dubbed ‘small-worlds’ [3], supporting a relational structure able to support both efficient system-wide communications [4, 5] and make them easy to navigate [6]. The efficient structural connectivity of these systems has a profound impact on their functionality, with the presence of shortcuts increasing the speed of contagion and the emergence of cooperation [7], and the ability of a system to synchronise [8]. For all these reasons, efficiently computing shortest paths in graphs is a problem that has attracted enormous interest in the research community for many decades [9], and it continues to do so.

The analysis of connectivity has also produced relevant insights in the case of temporal networks, where edges are not permanent but created and destroyed over time [10]. Structures such as paths [11] and connected components [12] have been formulated in the setting where network structure evolves over time, as well as numerous measures of centrality, [13]. The addition of a temporal dimension, in particular the presence of non-trivial temporal correlations [14] and memory [15] among interactions, has stimulated important research on increasingly complex temporal network models, able to reproduce empirical patterns [16–18]. Moreover, since the first observations about epidemic processes [19, 20], network temporality was found to have interesting consequences

also for the network dynamics, influencing the behaviour of individuals across a range of processes [21, 22].

Networks have classically modelled interactions through links, describing relations between pairs of entities only, even though in many real-world systems interactions simultaneously involve multiple nodes [23]. Recently, a wide variety of structural descriptors have been extended to account for the presence of such higher-order interactions, including algorithms for motif discovery [24] and analysis [25], community detection [26, 27], centrality measures [28], as well as network filtering [29] and reconstruction [30] procedures. Non-dyadic interactions generate new dynamical behaviours and collective phenomena [31, 32], from contagion [33, 34] to synchronisation [35–37] and evolutionary games [38, 39]. More recently, temporality has also been considered in higher-order networks, from burstiness [40] and temporal-topological correlations [41], to Markovian [42, 43] and non-Markovian [44, 45] structural models.

Despite these advances, characterising shortest paths and connectivity in systems with higher-order interactions remains an open problem. Recently, efforts have been devoted to characterise the concepts of distance [46] and walks [47] and networks in networks with non-dyadic ties, as well as proposing efficient algorithms [48] to extract shortest paths in hypergraphs, limiting the analysis to static systems.

In this work, we provide the first systematic investigation of the effect of higher-order interactions on system connectivity across a variety of real-world datasets. We quantify the contribution of non-dyadic ties for shortest path length, computing length distribution, average path size and the fraction of purely dyadic segments in each path, and show that all such features are compatible with a simple null-model which preserves the higher-order degree distribution. Next, we consider time-varying interactions, and extend the concept of higher-order path and components to temporal hypergraphs. Our analysis of multiple real-world systems reveals the crucial role of higher-order interactions to ensure efficient connectiv-

*Electronic address: bln1@st-andrews.ac.uk

†Electronic address: battistonf@ceu.edu

ity in temporal higher-order networks, characterises differences between topologically shortest and temporally fastest paths, and shows how the observed non-trivial empirical patterns can not be reproduced with simple randomised null-models. Our work provides new insights into the connectivity properties and the structural organisation of real-world hypergraphs, both for static and time-varying systems.

RESULTS

Data

To study shortest paths in temporal hypergraphs, we collected 25 publicly available datasets of real-world temporal systems with higher-order interactions. These hypergraphs describe social interactions from a broad range of domains such as households and schools, hospitals, workspaces and conferences, as well as political interactions between individuals in Congress and even contact data from baboons

| Dataset | V | E_{HO} | E_{DY} | $ e_{\max}^{HO} $ | T | dt |
|----------------|------|----------|----------|-------------------|-------|----------|
| Copenhagen | 692 | 449413 | 38088 | 21 | 8064 | 300s |
| Elem1 | 339 | 26543 | 14184 | 8 | 2244 | 20s |
| F&F: 2010-08 | 44 | 436 | 163 | 9 | 66 | 8h |
| F&F: 2010-09 | 58 | 1155 | 349 | 11 | 90 | 8h |
| F&F: 2010-10 | 128 | 4832 | 1293 | 13 | 90 | 8h |
| F&F: 2010-11 | 126 | 6094 | 1504 | 20 | 90 | 8h |
| F&F: 2010-12 | 121 | 4529 | 1091 | 21 | 90 | 8h |
| F&F: 2011-01 | 118 | 4070 | 1056 | 11 | 90 | 8h |
| F&F: 2011-02 | 117 | 6340 | 1268 | 20 | 90 | 8h |
| F&F: 2011-03 | 112 | 6529 | 1330 | 10 | 90 | 8h |
| F&F: 2011-04 | 112 | 6787 | 1320 | 16 | 90 | 8h |
| F&F: 2011-05 | 97 | 1257 | 364 | 8 | 18 | 8h |
| HS11 | 126 | 3642 | 151 | 44 | 610 | 20s |
| HS12 | 180 | 7458 | 378 | 46 | 1321 | 20s |
| InVS13 | 95 | 10502 | 2342 | 43 | 20129 | 20s |
| InVS15 | 219 | 35764 | 7846 | 71 | 21536 | 20s |
| Kenyan | 75 | 972 | 272 | 11 | 42 | 1hr |
| LH10 | 76 | 1854 | 1093 | 5 | 7639 | 20s |
| LyonSchool | 242 | 12704 | 7748 | 5 | 3100 | 20s |
| Malawi | 86 | 14051 | 194 | 24 | 1127 | 20s |
| Mid1 | 591 | 76062 | 49400 | 10 | 2505 | 20s |
| SFHH | 403 | 10541 | 8268 | 9 | 3509 | 1hr |
| Thiers13 | 327 | 7818 | 5498 | 5 | 7375 | 1hr |
| Baboons | 13 | 2892 | 78 | 13 | 1818 | 10 min |
| Congress Bills | 1718 | 82873 | 13845 | 25 | 5305 | 1 months |

TABLE I: Summary statistics of real-world temporal hypergraphs. V indicates the number of nodes, E_{HO} denotes the number of higher-order interactions and E_{DY} the number of purely dyadic interactions in the static system, and $|e_{\max}^{HO}|$ indicates the maximum size of a higher-order interaction. T measures the number of total timestamps and dt the interval between successive timestamps in the temporal hypergraphs.

We provide relevant summary statistics for the static

versions of each dataset in Table I, alongside the amount and resolution of successive timestamps for the temporal networks. A fuller description of the datasets is provided in Methods.

Static hypergraphs

In simple graphs, relational information is described by edges, which encode pairwise interactions between pairs of nodes only. A *path* is an ordered, non-repeating sequence of nodes, where each subsequent step occurs along a particular edge. Similarly, a hypergraph is a collection of nodes and hyperedges which encode interactions among an arbitrary number of nodes. The *size* of a hyperedge is defined as the number of nodes contained therein. A *hyperpath* or a *higher-order path* in a hypergraph is defined as an ordered, non-repeating sequence of nodes, where each subsequent step occurs between nodes within the same hyperedge.

The *length* of a higher-order path between any two nodes i and j , l_{ij} , is defined as the number of nodes it traverses minus 1. Intuitively, this may be thought of as the number of ‘steps’ taken. If no such path exists between 2 nodes, we set $l_{ij} = \infty$. Two nodes are *connected* if a path of finite length exists between them. While a pair of nodes can be connected by multiple distinct paths, the *shortest path* between any two nodes in a static network is defined as a path of minimum length, which might not necessarily be unique.

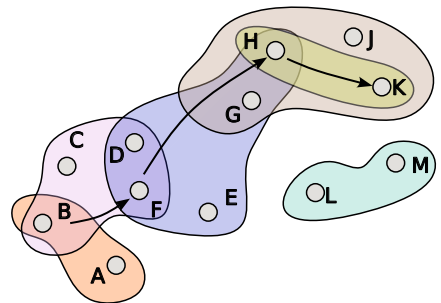


FIG. 1: The shortest hyperpath between nodes B and K has length $\ell = 3$ and average size $\langle s \rangle = (4 + 5 + 2)/3$.

Clearly, hyperpaths in higher-order networks will traverse hyperedges of varying sizes, where each segment of a hyperpath traverses a hyperedge of a potentially different size. As such, one may attach to each individual segment of a hyperpath its associated *size* s , defined as the size of the hyperedge that is traversed during that particular ‘step’. In some cases, such a step may be contained in multiple hyperedges, in which case we choose the hyperedge of smallest size to define its size. Paths in higher-order networks contain rich information and one may calculate the average size $\langle s \rangle$ of a path as the average size across traversed segments. For example, the average size of a path allows one to determine how much of a path

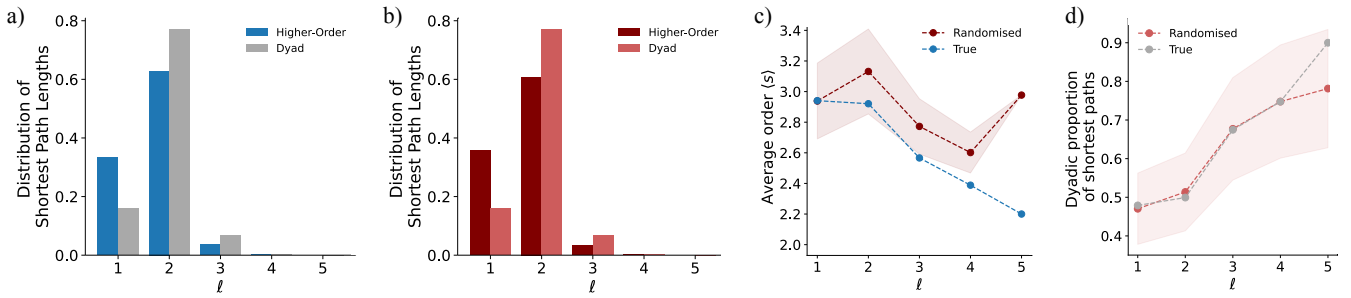


FIG. 2: Shortest paths in the static hypergraph of the Copenhagen study. Path-length distributions of higher-order and purely dyadic paths for hypergraphs of the Copenhagen dataset for (a) the empirical data and (b) a randomised null-model. (c) Average interaction size $\langle s \rangle$ of the higher-order path as a function of the path length for empirical (blue) and randomised (dark red) data. (d) Average fraction of each path which is purely dyadic as a function of the path length for empirical (grey) and randomised (light red) data. Shaded areas represent a 97.5% confidence interval obtained over 100 randomisations.

is composed of genuinely higher-order interactions. The minimum size of a path is $\langle s \rangle = 2$, which occurs when the hyperpath consists of purely pairwise interactions.

To illustrate these concepts, we consider the hypergraph in Figure 1. The shortest hyperpaths between nodes B and K have length $\ell = 3$. One of these is the hyperpath (B, F, H, K), where the segments (B, F), (F, H), and (H, K) have sizes 4, 5 and 2. The average size of such a hyperpath is then $\langle s \rangle = 11/3$. We note that the segment (H \rightarrow K) is also contained in a hyperedge of size four but that we select the hyperedge of minimum size to assign a size. Importantly, other shortest hyperpaths of the same length can exist. For instance, here the hyperpath (B, D, H, K) also has the same $\langle s \rangle = 11/3$. Another of such shortest hyperpaths is (B, D, G, K) which has a higher average size $\langle s \rangle = 13/3$.

We are interested in studying the higher-order organisation of shortest paths and the extent to which group interactions contribute to the forming of these paths in real-world systems.

We begin by considering static hypergraphs where we neglect information about the temporal nature of the interactions (see Methods for details). As an illustrative example, in Figure 2, we show results for the social hypergraph from the well-known Copenhagen network study, which describes social interactions over 4 weeks between 576 university students on a university campus.

In Figure 2a, we plot the distribution of shortest path lengths for higher-order paths in blue. We compare it with the distribution of path lengths of purely dyadic paths, obtained when taking considering only dyadic interactions, shown in grey. When higher-order interactions are not considered, we observe a distribution shift to the right, as such paths take longer to reach the same target as their higher-order counterparts. Interestingly, the same distributions of higher-order and dyadic path lengths are accurately reproduced by randomising the data with a higher-order configuration model (see Methods for details), as shown in Figure 2b.

Next, in Figure 2c, we study the average size $\langle s \rangle$ of shortest paths between connected nodes in the higher-order network as a function of their length ℓ . We observe that the shortest paths which are longer also tend to be those with a lower average size. This suggests that higher-order interactions are often central in the system, in agreement with recent work on hypercores [49] while dyadic edges remain crucial to connect more peripheral nodes. To further corroborate our intuition, in Figure 2d we plot the fraction of a shortest path that consists of purely dyadic segments, grouped by the length of the path itself. As expected, the curve is increasing, and such a behaviour is again well reproduced in the randomised system.

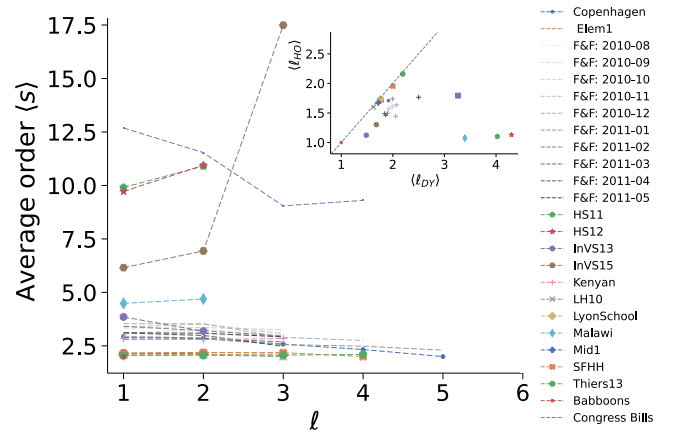


FIG. 3: Summary statistics for shortest paths in static hypergraphs. Average size $\langle s \rangle$ as a function of the path length across 25 datasets describing social interactions. (Inset) Average shortest higher-order path length $\langle \ell_{HO} \rangle$ against the average shortest dyadic path length $\langle \ell_{DY} \rangle$ for all datasets.

In Figure 3a we extend the analysis of higher-order shortest paths to all our datasets. We observe that the

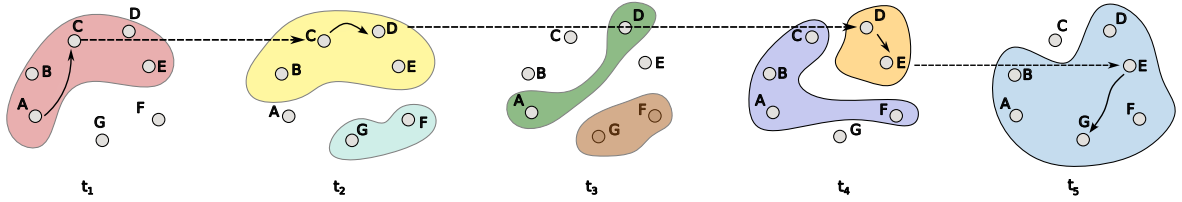


FIG. 4: Example of a temporal path travelling from node A at t_1 to node G at t_5 . The path has time duration $d = 5$ and path topological length $\ell = 4$.

average size $\langle s \rangle$ as a function of ℓ decreases in all systems, except for a dataset about social interactions in an office. Finally, in Figure 3b, for all datasets we show the difference in average path length for higher-order and purely dyadic paths. As expected, those systems which have $\langle s \rangle \approx 2$ in Figure 3a for all lengths are those which fall closest to the line $x = y$ in Figure 3b. Finally, we observe that the lengths of shortest paths in all datasets are very short, never having a length of more than 5, in agreement with the small-world nature of complex networks [3].

In summary, while higher-order interactions are important to ensure connectivity in static hypergraphs, in such a simple scenario most shortest path features can be reproduced by preserving the higher-order degree distribution. As we will see in the next section, a much richer picture emerges once we move beyond static systems and expand our analysis to consider the role of time.

Temporal hypergraphs

We model the temporal evolution of a networked system with a temporal network. A temporal network is a sequence of consecutive time-stamped static graphs, or alternatively a collection of nodes and a collection of timestamped edges. At any time t nodes can be active or inactive depending on whether they are participating in an interaction at that instance or not.

A temporal path is a sequence of interactions occurring at successive timestamps. More formally, a *temporal path* can be defined as an ordered sequence of (node, time) pairs, where consecutive pairs' timestamps must be increasing. An important consequence of temporality is that paths are not symmetric (even in the case of undirected graphs). In other words, the existence of a path from i to j does not imply the existence of a path from j to i and in general, even when both exist, they might be different and have different lengths. In this work, we assume that a message cannot be propagated further than its direct neighbours within any single snapshot (although the alternative makes sense when timestamps are at longer intervals), and that a node can 'retain' a message across multiple snapshots, following the approach of Ref. [13].

The concept of length in the temporal setting may be

defined in 2 complementary ways. The *temporal duration*, denoted d , of a temporal path from node i to node j is defined as the time elapsed between the activation time of node i and the first activation time of node j following the starting time. By contrast, the *length* or *step-count*, denoted ℓ , of a temporal path from nodes i to node j is defined as the total number of segments traversed and is equal to the number of nodes minus one.

Shortest temporal paths can therefore be either those that have minimum duration (d_{\min}), or minimum length (ℓ_{\min}). The *fastest path* (of shortest duration) between nodes i and j is the temporal path of minimum duration, and is set to infinity if such a path does not exist. The *shortest path* (with the fewest steps) counts the number of segments, and is hence analogous to the static case.

When a system describes time-varying interactions between groups of nodes, we use temporal hypergraphs. A *temporal hypergraph* is a sequence of static hypergraphs, indexed by time. The two notions of temporal length (duration and step count) can be defined as in the pairwise case. In Figure 4, a simple temporal hypergraph illustrates how such measures can differ. A temporal path $(A, t_1) \rightarrow (C, t_1) \rightarrow (D, t_2) \rightarrow (D, t_4) \rightarrow (E, t_4) \rightarrow (G, t_5)$ has a temporal length of 5, but a topological length of 4. In our temporal analysis, we mainly focus on fastest paths, and discuss differences with shortest paths in Figure 7.

We investigate temporal connectivity and fastest paths in various real-world systems to discover how much of the system's connectivity is due to higher-order interactions. Similarly to the static case, in Figure 5, we begin our exploration of the temporal connectivity properties of real-world systems by focusing on the Copenhagen dataset. In Figure 5a we plot side-by-side the distribution of durations of fastest paths across all interaction sizes in blue, and for only pairwise interactions in grey. We note that the duration of such paths can be very long, even well above 100 time units. When only pairwise interactions are considered, there is a distinct distribution shift to the right of temporal path lengths. Such an effect of higher-order interactions is much greater than what we observed for the path length in static hypergraphs, making explicit the very relevant role of non-dyadic connections in determining the connectivity properties of temporal systems.

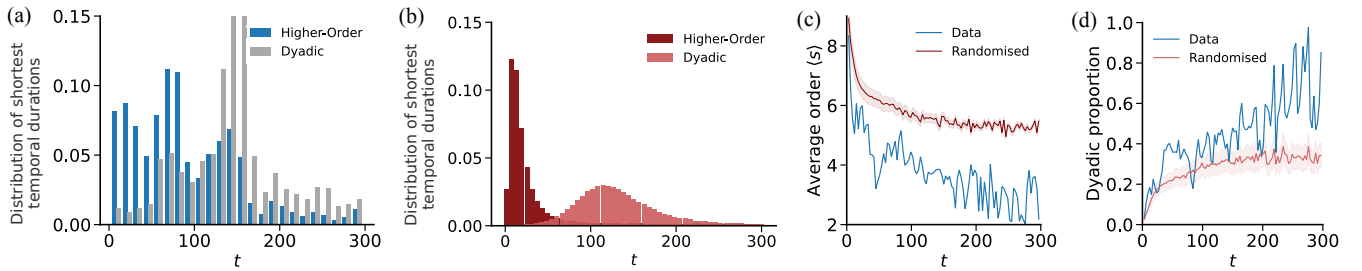


FIG. 5: Fastest paths in the temporal hypergraph of the Copenhagen study. Path-duration distributions of higher-order and purely dyadic paths for hypergraphs of the Copenhagen dataset for (a) the empirical data and (b) a randomised null-model. (c) Average interaction size $\langle s \rangle$ of the higher-order path as a function of the path duration for empirical (blue) and randomised (dark red) data. (d) Average fraction of each path which is purely dyadic as a function of the path duration for empirical (grey) and randomised (light red) data. Shaded areas represent a 97.5% confidence interval obtained over 100 randomisations.

In Figure 5b we plot the same distribution of durations for a randomisation of the data where hyperedges’ time-information is shuffled but the underlying static graph is kept constant. As shown, such a randomisation fails to reproduce the distribution of durations of the actual system, as washing out temporal correlations among hyperedges makes the typical duration of fastest paths in the null model much shorter and narrower than in the true data.

Next, in Figure 5c we plot the average size $\langle s \rangle$ of fastest paths between connected nodes in the higher-order network, grouped by their duration, for both real and randomised data. As in the static case, we observe that paths that last longer also tend to have a lower average size in both the true and randomised networks. Faster paths traverse more higher-order interactions. In contrast, paths with longer duration use more dyadic edges, as illustrated in Figure 5d, which shows the average fraction of fastest paths composed of pure dyadic interactions, grouped by path duration. While the null model qualitatively reproduces the observed trends, we observe that fastest paths in the randomised data systematically underestimate the usage of dyadic edges in temporal paths.

In Figure 6a we broaden our investigation to consider fastest paths for all datasets in our collection and plot $\langle s \rangle$ against t , the number of timesteps across all datasets. Again, we observe again the same downward trend of decreasing average size with increasing path duration which is even more pronounced when plotting the topological length of fastest paths, and an increasing dyadic proportion for longer path lengths (last two not shown here). In Figure 6b, we compare fastest higher-order path durations d_{HO} with fastest dyadic path durations d_{DY} , calculating the percentage of pairs of nodes that are only connected if they may traverse group interactions. While there is variability across real-world systems, we observe that in many cases a high percentage of paths disappear when only true dyadic segments are considered, highlighting the importance of higher-order interactions for

the global architecture of the system. For those nodes that remained connected even when only dyadic interactions were allowed, in Figure 6c, we visualise how much longer on average a dyadic temporal path will tend to be than its higher-order counterpart. We note that in some cases such differences can be very large, such as for the InVS13 and the Baboons datasets.

| Datasets | NCC | | LCC | |
|-------------|--------|----------|--------|----------|
| | Static | Temporal | Static | Temporal |
| Baboons | 1 | 14 | 1.00 | 0.62 |
| Malawi | 1 | 30720 | 1.00 | 0.35 |
| LH10 | 1 | 4 | 1.00 | 0.13 |
| F&F 2010-10 | 1 | 96 | 1.00 | 0.27 |
| F&F 2010-08 | 2 | 992 | 0.95 | 0.39 |
| F&F 2010-09 | 1 | 128 | 1.00 | 0.31 |
| Kenyan | 3 | 692 | 0.41 | 0.17 |
| Thiers13 | 1 | 50 | 1.00 | 0.01 |

TABLE II: Connected components in static and temporal hypergraphs. The first column presents the number of connected and temporally strongly connected components (NCC) for static and temporal versions of the dataset. The second column gives the relative size of the largest connected and strongly temporally connected components ($|LCC|$) when counting included nodes.

Path temporality also has consequences for the concept of connected components. Following Ref. [12], we define two nodes as *strongly temporally connected* if there is a temporal path from i to j and also vice versa. A *temporal strongly connected component* is the set of vertices for which any participating node can both reach and be reached by all other nodes in the set. To quantify the reachability of nodes in the systems, we study the temporal connectivity of the datasets in Table II by calculating the number of the strongly connected temporal components and the size of the largest. We compare this with the number and largest size of connected components in the static network. The temporal calculation is known to be an NP-complete problem [13] which is only compu-

tationally feasible for smaller graphs, so we present here results only for those networks that we were able to compute. We observe that the static hypergraph for nearly all datasets has a single giant connected component containing all nodes. In contrast, the temporal systems will be much more fractured, with components that are more numerous and smaller in size.

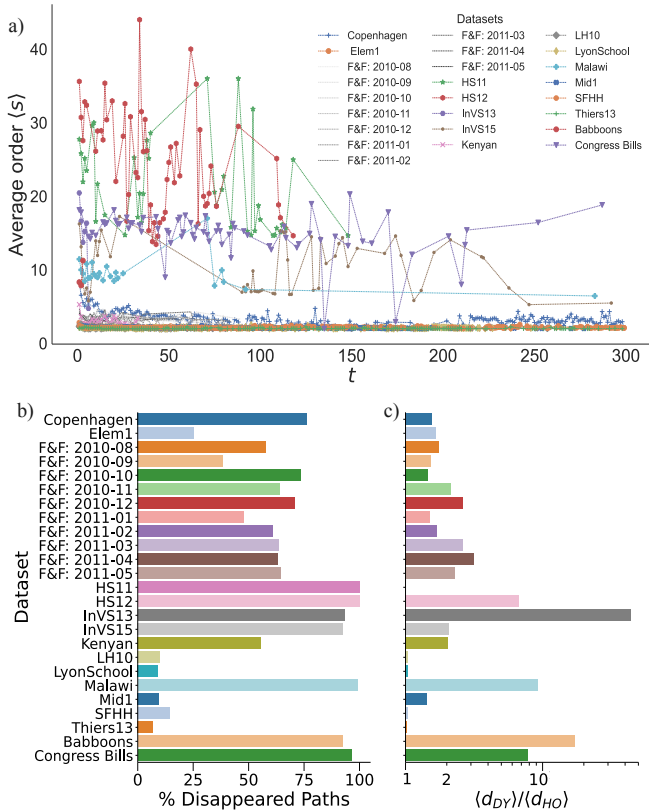


FIG. 6: Features of fastest paths in temporal hypergraphs. Average size $\langle s \rangle$ as a function of the path length across all datasets (a). For each dataset, we also show the percentage of fastest paths that only exist as higher-order paths (b), and how much longer in duration the dyadic paths are than the original higher-order paths on average (c).

Finally, in Figure 7 we investigate the differences between path duration between fastest (F) and topologically shortest (S) temporal path, as defined at the beginning of this section. In Figure 7a we plot the percentage of higher-order paths that differ between fastest and shortest for each dataset. We then determine how much longer shortest paths last than fastest paths by computing the fraction $\langle d_{\min}^S \rangle / \langle d_{\min}^F \rangle$ in Figure 7b. As shown, many of the fastest paths are not topologically shortest, with this phenomenon having different intensities in different systems. For instance, in the Copenhagen dataset we reach the highest percentage of different fastest versus topologically shortest temporal paths among pairs of nodes, with this number being close to 60%, while in a

social hypergraph of interactions among baboons, fastest and shortest paths are almost always the same. In Figure 7b we quantify how much longer shortest paths takes instead of fastest ones across real-world systems by computing the ratio between their average durations. While in some cases topologically shortest paths are on average only a little slower than fastest ones, as in the case of a Sociopatterns data of social interactions in a high school ($\langle d_{\min}^S \rangle / \langle d_{\min}^F \rangle = 1.1$), in some other cases the duration of shortest paths can be twice as much as that of fastest ones, as for the Congress Bills dataset.

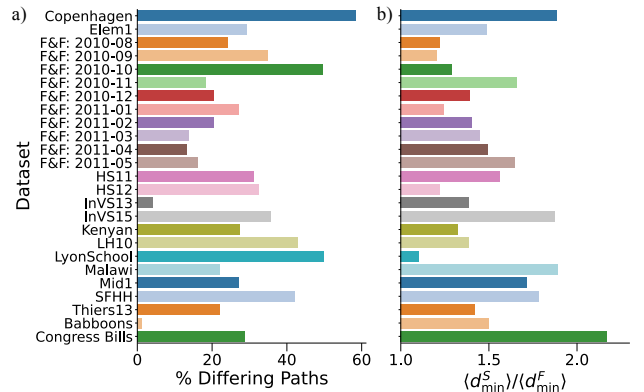


FIG. 7: Comparing fastest versus shortest in temporal hypergraphs. For each dataset, we show the percentage of paths that differ between shortest and fastest across all pairs of individuals (a), and how much faster on average the fastest path is when compared to the shortest path (b).

CONCLUSION

In this work we have unveiled the higher-order organization of shortest paths in systems with non-dyadic interactions. By investigating average path size in many real-world hypergraphs, higher-order interactions are crucial to introduce shortcuts into the system, enabling efficient communications beyond system units that would otherwise be disconnected if only pairwise segments were considered. We extended our analysis to the case of temporal hypergraphs, investigating both temporally fastest and topologically shortest paths showing how real-world connectivity cannot be reproduced by simple randomised null models.

Analysing large higher-order temporal networks by calculating all shortest/fastest paths has a very high computational cost, as it requires global information about the system. This makes the analysis particularly hard for very dense networks, such as the Copenhagen Network Study, or very large ones. In order to analyse larger systems, it would be important to develop more efficient methods, for instance based on the development of heuristics for higher-order networks that would allow

the calculation of the shortest path lengths in an approximate but more efficient way, similar to what was recently done for the problem of higher-order motifs [50]. Another possible extension of the work would be to investigate the effect of the size of the time window considered in our calculations on the emerging connectivity, as previously done for the case of burstiness [19, 40]. Finally, our results might be used to develop alternative attack strategies to dismantle the system by affecting shortest paths and flow. Our work investigates the connectivity properties of static and time-varying hypergraphs, contributing to a better understanding of the structural organisation of systems with higher-order interactions.

METHODS

Datasets

This section provides more detailed descriptions of the 25 datasets used in the above analyses.

Thirteen of the datasets [51–54] (*Copenhagen*, *Friends & Family* (monthly between August 2010 - May 2011), *Kenyan*, *Malawi*) describe generic face-to-face interactions between individuals. The Friends & Family dataset is particularly rich as it spans an extended time period while simultaneously storing information at a very high time resolution. We therefore opt to split it into 10 smaller datasets, each tracking the temporal evolution over one calendar month. Additionally, following the procedure for intermediate aggregation as described below, we group time frames into blocks of 8 hours and create a static hypergraph for each interval.

Six of the datasets [55–57] (*LyonSchool* and *Thiers13*, *HS11* and *HS12*, *Elem1* and *Mid1*) describe interactions between pupils at school. Five datasets [55, 58, 59] describe interaction patterns within diverse work environments, namely a hospital (*LH10*, *DAWN*), a workspace (*InVS13* and *InVS15*) and a conference (*SFHH*). For all of these datasets, nodes correspond to individuals and hyperedges correspond to group interactions.

One dataset [60] records contact data between baboons (*Baboons*) and each hyperedge is a maximal clique within an specific interval of the temporal network of contacts.

The final dataset (*Congress-bills*) describes political interactions between the US House of Representatives and Senate [59]. Nodes here represent congresspersons and each hyperedge contains all sponsors and co-sponsors of a specific legislative bill.

Higher-order reconstruction and aggregation

We use 25 freely available datasets for our analyses describing group interactions. Even though interactions involve groups, the majority of the datasets store interactions between individuals as (time, node, node)-tuples as

a computational simplification even when interactions involve groups. We are here interested in investigating the different contributions of higher-order and dyadic edges to the higher-order organisation of networks. To this end, we assume that if k individuals are all pairwise connected at time t (i.e. they form a clique), then together they form a group of size k and are promoted to a hyperedge of size k in the temporal hypergraph.

Throughout our analyses, we distinguish between ‘true’ dyadic interactions and those which are an artefact of the data structures chosen to store the data digitally. We consider an edge to be a ‘pure pairwise’ interaction when it does not form part of any larger clique, i.e. when it cannot be promoted to a group.

We create the static hypergraph by omitting temporal information and generating a hypergraph with all nodes and interactions reported. In effect, this collates all snapshots into a single network. This allows for potentially nested edges to exist in cases where a group of individuals at one time lose/gain members at an earlier/later time, even though in general we assume nested edges do not exist due to the way in which we create hyperedges.

To investigate the temporal evolution of social systems, we construct a temporal network as a sequence of static hypergraphs, each associated with a specific timestamp. In some datasets we have very fine-grained temporal information, with data logged at intervals of between 20s-5mins. This implies that many of the static snapshots have very few edges. We accordingly perform a preprocessing step and aggregate across bigger windows (e.g. grouping together snapshots of resolution 30s into groups of 5 minutes). This means that even for a temporal network, some static hypergraph snapshots may include nested hyperedges. The choice of aggregation window is determined in a data-driven manner by plotting the size of the largest connected component as a function of the size of the aggregation window and taking note of when its size saturates. We select the smallest window for which the largest connected component no longer grows.

The duration of a temporal path from node i at some time t_1 to node j is defined as the time elapsed between the activation time of node i at t_1 and the first time t_2 that node j becomes active after t_1 . If multiple shortest/fastest paths exist between a pair of nodes, we select a single path uniformly and at random. When assigning sizes to the segments of a path there may be ambiguity when the segment forms part of more than one hyperedge. In this case, we select the hyperedge of minimum size and assign to the segment its size. This is inspired by the notion that smaller groups will tend to be more capable of accurately transmitting information.

Calculating minimum-length paths

Calculating fastest paths in temporal networks is a non-trivial task. To enable us to calculate time-respecting paths, we first map a temporal higher-order

network to a static digraph representation whose nodes are now tuples of (time, node) pairs from the original temporal hypergraph [61, 62]. We may then easily extract temporal paths from this new digraph. To calculate minimum-length topological paths, we assign a weight of 1 to all edges and employ Dijkstra’s shortest path algorithm [63]. To calculate minimum-duration temporal paths, we weight edges by the time interval traversed and again use Dijkstra’s algorithm. As before, in the presence of multiple paths we resolve ambiguities by picking one uniformly and at random. If a node ‘stores’ a message across t timesteps of length dt , this node is considered to contribute $t \cdot dt$ units to the temporal path length.

Moreover, calculating shortest paths for large networks is computationally expensive, so we opt to pick a starting time t_0 and window length w and label V_{t_0} as the starting node-set. In our case, all datasets have a window size of 300 timesteps, except for the Friends & Family dataset, which spans the entire calendar month. We then determine the existence and length of fastest and shortest paths from this starting set V_{t_0} to all other nodes in the set V within a timeframe of w consecutive time snapshots. As before, non-existent paths are set to have a path length of ∞ .

Because the datasets all have different time intervals, and to enable comparison of temporal path lengths across datasets, we consider only the number of timesteps for the information reported in Figures 5-7.

Randomisations

We consider randomisations of the data in both the static and temporal settings to compare our results. For

both cases we generate 100 realisations of the particular null model and plot the resulting averages and 97.5% confidence intervals in the figures. For the static hypergraph, we use the higher-order configuration model, an extension of the well-known configuration model that keeps the degree-distribution fixed across all orders and generates a new edge-set. For temporal hypernetworks, we use a randomisation that shuffles the timestamps of instantaneous events inside individual timelines to create a rearranged version while still preserving both the underlying static hypergraph and the total number of events, following the methodology of [64].

CODE AVAILABILITY

The code to perform the analyses described will soon be publicly available as implemented functions within HypergraphX [65], an open-source Python library for higher-order network analysis.

DATA AVAILABILITY

The datasets are public and their associated preprocessing will be made publicly available online at <https://github.com/joanne-b-nortier/higher-order-shortest-paths>.

-
- [1] Mark Newman. *Networks*. Oxford University Press, 07 2018.
 - [2] Michael Molloy and Bruce Reed. A critical point for random graphs with a given degree sequence. *Random structures & algorithms*, 6(2-3):161–180, 1995.
 - [3] Duncan J Watts and Steven H Strogatz. Collective dynamics of ‘small-world’ networks. *nature*, 393(6684):440–442, 1998.
 - [4] Vito Latora and Massimo Marchiori. Efficient behavior of small-world networks. *Physical review letters*, 87(19):198701, 2001.
 - [5] Ernesto Estrada and Naomichi Hatano. Communicability in complex networks. *Physical Review E—Statistical, Nonlinear, and Soft Matter Physics*, 77(3):036111, 2008.
 - [6] Jon M Kleinberg. Navigation in a small world. *Nature*, 406(6798):845–845, 2000.
 - [7] Francisco C Santos, João F Rodrigues, and Jorge M Pacheco. Epidemic spreading and cooperation dynamics on homogeneous small-world networks. *Physical Review E—Statistical, Nonlinear, and Soft Matter Physics*, 72(5):056128, 2005.
 - [8] Mauricio Barahona and Louis M Pecora. Synchronization in small-world systems. *Physical review letters*, 89(5):054101, 2002.
 - [9] Edsger W Dijkstra. A note on two problems in connexion with graphs. In *Edsger Wybe Dijkstra: his life, work, and legacy*, pages 287–290. 2022.
 - [10] Petter Holme and Jari Saramäki. Temporal networks. *Physics reports*, 519(3):97–125, 2012.
 - [11] Huanhuan Wu, James Cheng, Silu Huang, Yiping Ke, Yi Lu, and Yanyan Xu. Path problems in temporal graphs. *Proceedings of the VLDB Endowment*, 7(9):721–732, 2014.
 - [12] Vincenzo Nicosia, John Tang, Mirco Musolesi, Giovanni Russo, Cecilia Mascolo, and Vito Latora. Components in time-varying graphs. *Chaos: An interdisciplinary journal of nonlinear science*, 22(2), 2012.
 - [13] Vincenzo Nicosia, John Tang, Cecilia Mascolo, Mirco Musolesi, Giovanni Russo, and Vito Latora. Graph metrics for temporal networks. *Temporal networks*, pages 15–40, 2013.
 - [14] Márton Karsai, Kimmo Kaski, Albert-László Barabási, and János Kertész. Universal features of correlated bursty behaviour. *Scientific reports*, 2(1):397, 2012.

- [15] Oliver E Williams, Lucas Lacasa, Ana P Millán, and Vito Latora. The shape of memory in temporal networks. *Nature communications*, 13(1):499, 2022.
- [16] Nicola Perra, Bruno Gonçalves, Romualdo Pastor-Satorras, and Alessandro Vespignani. Activity driven modeling of time varying networks. *Scientific reports*, 2(1):469, 2012.
- [17] Lucas Lacasa, Jorge P Rodriguez, and Victor M Eguiluz. Correlations of network trajectories. *Physical Review Research*, 4(4):L042008, 2022.
- [18] Oliver E Williams, Piero Mazzarisi, Fabrizio Lillo, and Vito Latora. Non-markovian temporal networks with auto-and cross-correlated link dynamics. *Physical Review E*, 105(3):034301, 2022.
- [19] Márton Karsai, Mikko Kivelä, Raj Kumar Pan, Kimmo Kaski, János Kertész, A-L Barabási, and Jari Saramäki. Small but slow world: How network topology and burstiness slow down spreading. *Physical Review E—Statistical, Nonlinear, and Soft Matter Physics*, 83(2):025102, 2011.
- [20] Luis EC Rocha, Fredrik Liljeros, and Petter Holme. Simulated epidemics in an empirical spatiotemporal network of 50,185 sexual contacts. *PLoS computational biology*, 7(3):e1001109, 2011.
- [21] Ingo Scholtes, Nicolas Wider, René Pfitzner, Antonios Garas, Claudio J Tessone, and Frank Schweitzer. Causality-driven slow-down and speed-up of diffusion in non-markovian temporal networks. *Nature communications*, 5(1):5024, 2014.
- [22] Michele Starnini, James P Gleeson, and Marián Boguñá. Equivalence between non-markovian and markovian dynamics in epidemic spreading processes. *Physical review letters*, 118(12):128301, 2017.
- [23] Federico Battiston, Giulia Cencetti, Iacopo Iacopini, Vito Latora, Maxime Lucas, Alice Patania, Jean-Gabriel Young, and Giovanni Petri. Networks beyond pairwise interactions: Structure and dynamics. *Physics reports*, 874:1–92, 2020.
- [24] Quintino Francesco Lotito, Federico Musciotto, Alberto Montresor, and Federico Battiston. Higher-order motif analysis in hypergraphs. *Communications Physics*, 5(1):79, 2022.
- [25] Peter Mann, V. Anne Smith, John B. O. Mitchell, and Simon Dobson. Random graphs with arbitrary clustering and their applications. *Phys. Rev. E*, 103:012309, Jan 2021.
- [26] Anton Eriksson, Timoteo Carletti, Renaud Lambiotte, Alexis Rojas, and Martin Rosvall. Flow-based community detection in hypergraphs. In *Higher-Order Systems*, pages 141–161. Springer, 2022.
- [27] Nicolò Ruggeri, Martina Contisciani, Federico Battiston, and Caterina De Bacco. Community detection in large hypergraphs. *Science Advances*, 9(28):eadg9159, 2023.
- [28] Austin R Benson. Three hypergraph eigenvector centralities. *SIAM Journal on Mathematics of Data Science*, 1(2):293–312, 2019.
- [29] Federico Musciotto, Federico Battiston, and Rosario N Mantegna. Detecting informative higher-order interactions in statistically validated hypergraphs. *Communications Physics*, 4(1):218, 2021.
- [30] Jean-Gabriel Young, Giovanni Petri, and Tiago P Peixoto. Hypergraph reconstruction from network data. *Communications Physics*, 4(1):135, 2021.
- [31] Federico Battiston, Enrico Amico, Alain Barrat, Ginestra Bianconi, Guilherme Ferraz de Arruda, Benedetta Franceschiello, Iacopo Iacopini, Sonia Kéfi, Vito Latora, Yamir Moreno, et al. The physics of higher-order interactions in complex systems. *Nature Physics*, 17(10):1093–1098, 2021.
- [32] Christian Bick, Elizabeth Gross, Heather A Harrington, and Michael T Schaub. What are higher-order networks? *SIAM Review*, 65(3):686–731, 2023.
- [33] Iacopo Iacopini, Giovanni Petri, Alain Barrat, and Vito Latora. Simplicial models of social contagion. *Nature communications*, 10(1):2485, 2019.
- [34] Guilherme Ferraz de Arruda, Giovanni Petri, and Yamir Moreno. Social contagion models on hypergraphs. *Physical Review Research*, 2(2):023032, 2020.
- [35] Per Sebastian Skardal and Alex Arenas. Higher order interactions in complex networks of phase oscillators promote abrupt synchronization switching. *Communications Physics*, 3(1):218, 2020.
- [36] Ana P Millán, Joaquín J Torres, and Ginestra Bianconi. Explosive higher-order kuramoto dynamics on simplicial complexes. *Physical Review Letters*, 124(21):218301, 2020.
- [37] Yuanzhao Zhang, Maxime Lucas, and Federico Battiston. Higher-order interactions shape collective dynamics differently in hypergraphs and simplicial complexes. *Nature communications*, 14(1):1605, 2023.
- [38] Unai Alvarez-Rodriguez, Federico Battiston, Guilherme Ferraz de Arruda, Yamir Moreno, Matjaž Perc, and Vito Latora. Evolutionary dynamics of higher-order interactions in social networks. *Nature Human Behaviour*, 5(5):586–595, 2021.
- [39] Andrea Civilini, Onkar Sadekar, Federico Battiston, Jesús Gómez-Gardeñes, and Vito Latora. Explosive cooperation in social dilemmas on higher-order networks. *Physical Review Letters*, 132(16):167401, 2024.
- [40] Giulia Cencetti, Federico Battiston, Bruno Lepri, and Márton Karsai. Temporal properties of higher-order interactions in social networks. *Scientific reports*, 11(1):7028, 2021.
- [41] Alberto Ceria and Huijuan Wang. Temporal-topological properties of higher-order evolving networks. *Scientific Reports*, 13(1):5885, 2023.
- [42] Giovanni Petri and Alain Barrat. Simplicial activity driven model. *Physical review letters*, 121(22):228301, 2018.
- [43] Leonardo Di Gaetano, Federico Battiston, and Michele Starnini. Percolation and topological properties of temporal higher-order networks. *Physical Review Letters*, 132(3):037401, 2024.
- [44] Luca Gallo, Lucas Lacasa, Vito Latora, and Federico Battiston. Higher-order correlations reveal complex memory in temporal hypergraphs. *Nature Communications*, 15(1):4754, 2024.
- [45] Iacopo Iacopini, Márton Karsai, and Alain Barrat. The temporal dynamics of group interactions in higher-order social networks. *Nature Communications*, 15(1):7391, 2024.
- [46] Ekaterina Vasilyeva, Miguel Romance, Ivan Samoylenko, Kirill Kovalenko, Daniil Musatov, Andrey Mihailovich Raigorodskii, and Stefano Boccaletti. Distances in higher-order networks and the metric structure of hypergraphs. *Entropy*, 25(6), 2023.
- [47] Sinan G Aksoy, Cliff Joslyn, Carlos Ortiz Marrero, Brenda Praggastis, and Emilie Purvine. Hypernetwork

- science via high-order hypergraph walks. *EPJ Data Science*, 9(1):16, 2020.
- [48] Jianhang Gao, Qing Zhao, Wei Ren, Ananthram Swami, Ram Ramanathan, and Amotz Bar-Noy. Dynamic shortest path algorithms for hypergraphs. *IEEE/ACM Transactions on Networking*, 23(6):1805–1817, 2015.
- [49] Marco Mancastroppa, Iacopo Iacopini, Giovanni Petri, and Alain Barrat. The structural evolution of temporal hypergraphs through the lens of hyper-cores. *arXiv preprint arXiv:2402.06485*, 2024.
- [50] Quintino Francesco Lotito, Federico Musciotto, Federico Battiston, and Alberto Montresor. Exact and sampling methods for mining higher-order motifs in large hypergraphs. *Computing*, 106(2):475–494, 2024.
- [51] Piotr Sapiezynski, Arkadiusz Stopczynski, David Dreyer Lassen, and Sune Lehmann. Interaction data from the copenhagen networks study. *Scientific Data*, 6(1):315, 2019.
- [52] Nadav Aharony, Wei Pan, Cory Ip, Inas Khayal, and Alex Pentland. Social fmri: Investigating and shaping social mechanisms in the real world. *Pervasive and mobile computing*, 7(6):643–659, 2011.
- [53] MC Kiti, M Tizzoni, TM Kinyanjui, DC Koech, PK Munywoki, M Meriac, L Cappa, A Panisson, A Barrat, C Cattuto, et al. Quantifying social contacts in a household setting of rural kenya using wearable proximity sensors. *epj data sci* 5: 21, 2016.
- [54] Laura Ozella, Daniela Paolotti, Guilherme Lichand, Jorge P Rodríguez, Simon Haenni, John Phuka, Onicio B Leal-Neto, and Ciro Cattuto. Using wearable proximity sensors to characterize social contact patterns in a village of rural malawi. *EPJ Data Science*, 10(1):46, 2021.
- [55] M Génois and A Barrat. Can co-location be used as a proxy for face-to-face contacts? *epj data sci* 7 (1): 11, 2018.
- [56] Julie Fournet and Alain Barrat. Contact patterns among high school students. *PLoS one*, 9(9):e107878, 2014.
- [57] Damon JA Toth, Molly Leecaster, Warren BP Pettey, Adi V Gundlapalli, Hongjiang Gao, Jeanette J Rainey, Amra Uzicanin, and Matthew H Samore. The role of heterogeneity in contact timing and duration in network models of influenza spread in schools. *Journal of The Royal Society Interface*, 12(108):20150279, 2015.
- [58] Austin R Benson, Rediet Abebe, Michael T Schaub, Ali Jadbabaie, and Jon Kleinberg. Simplicial closure and higher-order link prediction. *Proceedings of the National Academy of Sciences*, 115(48):E11221–E11230, 2018.
- [59] James H Fowler. Legislative cosponsorship networks in the us house and senate. *Social networks*, 28(4):454–465, 2006.
- [60] Valeria Gelardi, Jeanne Godard, Dany Paleressompouille, Nicolas Claidiere, and Alain Barrat. Measuring social networks in primates: wearable sensors versus direct observations. *Proceedings of the Royal Society A*, 476(2236):20190737, 2020.
- [61] Eugenio Valdano, Luca Ferreri, Chiara Poletto, and Vittoria Colizza. Analytical computation of the epidemic threshold on temporal networks. *Physical Review X*, 5(2):021005, 2015.
- [62] Koya Sato, Mizuki Oka, Alain Barrat, and Ciro Cattuto. Dyane: dynamics-aware node embedding for temporal networks. *arXiv preprint arXiv:1909.05976*, 2019.
- [63] Thomas H Cormen. Section 24.3: Dijkstra’s algorithm. *Introduction to algorithms*, pages 595–601, 2001.
- [64] Laetitia Gauvin, Mathieu Génois, Márton Karsai, Mikko Kivela, Taro Takaguchi, Eugenio Valdano, and Christian L Vestergaard. Randomized reference models for temporal networks. *SIAM Review*, 64(4):763–830, 2022.
- [65] Quintino Francesco Lotito, Martina Contisciani, Caterina De Bacco, Leonardo Di Gaetano, Luca Gallo, Alberto Montresor, Federico Musciotto, Nicolò Ruggeri, and Federico Battiston. Hypergraphx: a library for higher-order network analysis. *Journal of Complex Networks*, 11(3):cnad019, 2023.